Neuron, Vol. 41, 405–415, February 5, 2004, Copyright ©2004 by Cell Press

PKC Signaling Mediates Global Enhancement of Excitatory Synaptogenesis in Neurons Triggered by Local Contact with Astrocytes

Hiroshi Hama,[1,3] Chikako Hara,[1,3] Kazuhiko Yamaguchi,[2,3] and Atsushi Miyawaki[1,3,*]
[1]Laboratory for Cell Function Dynamics
Advanced Technology Development Group
[2]Laboratory for Learning and Memory
Brain Science Institute
RIKEN, 2-1 Hirosawa
Wako-City, Saitama, 351-0198
[3]CREST
Japan Science and Technology Corporation
Kawaguchi, Saitama 332-0012
Japan

Summary

Here we provide evidence that astrocytes affect neuronal synaptogenesis by the process of adhesion. Local contact with astrocytes via integrin receptors elicited protein kinase C (PKC) activation in individual dissociated neurons cultured in astrocyte-conditioned medium. This activation, initially focal, soon spread throughout the entire neuron. We then demonstrated pharmacologically that the arachidonic acid cascade, triggered by the integrin reception, is responsible for the global activation of PKC. Local astrocytic contact also facilitated excitatory synaptogenesis throughout the neuron, a process which could be blocked by inhibitors of both integrins and PKC. Thus, propagation of PKC signaling represents an underlying mechanism for global neuronal maturation following local astrocyte adhesion.

Introduction

Astrocytes have traditionally been considered passive bystanders in the formation and operation of neural circuitry. Accumulating evidence, however, suggests that these cells are in fact active participants in the creation and control of synapses (Haydon, 2001). Although the co-culture of purified neurons with astrocytes can facilitate synaptogenesis, it is unclear whether diffusible or membrane-bound astrocyte-derived factors were responsible for this increase in synaptogenetic efficiency (Pfrieger and Barres, 1997). Previous studies showed that an astrocyte-derived signal released into the medium induces the maturation of retinal ganglion cells (Ullian et al., 2001); this diffusible factor was identified as cholesterol complexed with apolipoprotein E-containing lipoproteins (Mauch et al., 2001). As synaptogenesis entails the formation of a large quantity of membrane structures (such as synaptic vesicles), the availability of astrocyte-produced cholesterol may serve to limit synapse development. It has also been reported that astrocyte-released L-serine and glycine promote survival, dendritogenesis, and the electrophysiological development of cultured cerebellar Purkinje neurons (Furuya et al., 2000).

*Correspondence: matsushi@brain.riken.go.jp

Nevertheless, it remains unknown if astrocyte membrane-bound factors also promote synaptogenesis. To address this question, we overlaid mature astrocytes onto isolated hippocampal neurons grown on spots of permissive substrate, and examined synapse formation. The continual supplementation of the medium with astrocyte-derived diffusible factors allowed us to distinguish contact effects from trophic effects. Here we demonstrate that local contact with astrocytes promotes global synaptogenesis, with PKC signaling responsible for signal propagation.

Results

Astrocyte Overlay on Isolated Neurons

To examine the effects of astrocyte adhesion on neuronal maturation, rat hippocampal neurons were grown in isolation in astrocyte-conditioned medium. A solution mist containing poly L-lysine and collagen was sprinkled onto agarose-coated glass coverslips, generating well-separated microislands (Figure 1A). Microisland size was generally uniform, with diameters ranging from 100 to 150 μm, each large enough to accommodate one to two plated neurons prepared from embryonic rat brain (Figure 1B). Confluent astrocytes were also present in the cultures, but were restricted to the rims of culture dishes (Figure 1A). As a result, the medium was continuously supplemented with astrocyte-derived diffusible factors, enabling isolated neurons both to survive for over two weeks and to form synapses between their own processes (autapses) (Bekkers and Stevens, 1991) to some degrees. Without bystander astrocytes, the purified neurons could not survive longer than 3 days after plating. After 8–9 days in culture, the neurons were overlaid with astrocytes (Astrocyte Plus) or left in culture with astrocytes at the periphery (Control). A typical encounter is shown in Figure 1C. Astrocyte plasma membranes were labeled with a fusion of GFP and the 22 amino acid N terminus of the Lyn receptor tyrosine kinase (Lyn-GFP) (Sawano et al., 2002). After 10–15 min, astrocytes began to move along the neurites while dynamically changing shape, as seen in the time-lapse image (Figure 1D; a full sequence is shown in Supplemental Figure S1 at http://www.neuron.org/cgi/content/full/41/3/405/DC1). Within 24 hr, the astrocyte settled down, remaining on one face of the neuron. Throughout the 2 day observation period in all cases, a significant fraction of the neuronal surface remained untouched by the astrocyte.

Maturation of Presynaptic Terminals by Astrocyte Overlay

Under these experimental conditions, any observed differences between Astrocyte Plus and Control neurons can be directly ascribed to contact effects of the overlaid astrocytes, as both are exposed to diffusible astrocyte-derived factors. Incubation of neurons with overlaid astrocytes for 2 days significantly augmented FM4-64 staining at the processes (Supplemental Figure S2 at

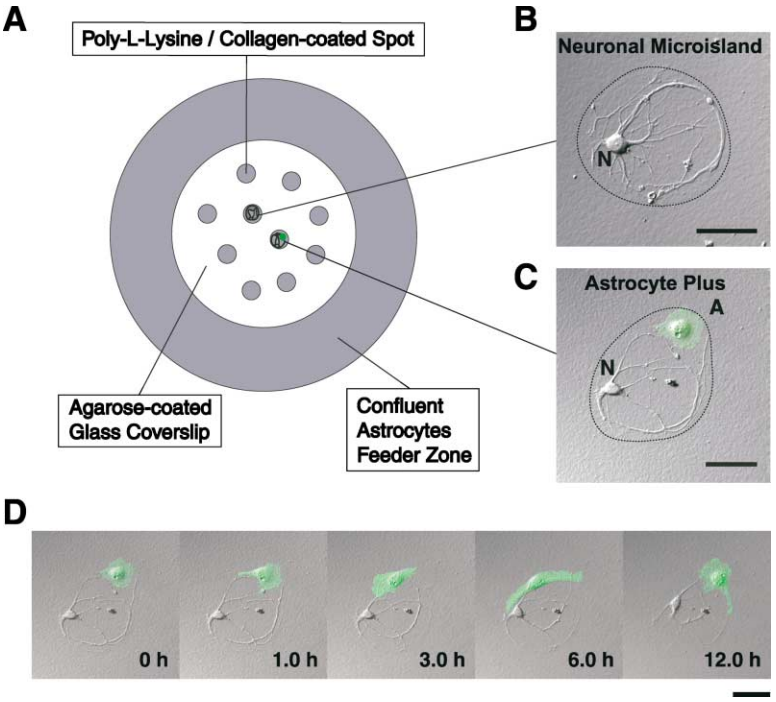

Figure 1. Microisland Culture for the Visualization of Interactions between Purified Neurons and Overlaid Astrocytes

(A) A schematic top view of a 35 mm dish. Confluent astrocytes were kept at the periphery. In the center of the dish, microislands of poly-L-lysine and collagen were scattered onto an agarose-coated coverslip.

(B) Micrograph of a neuron on a microisland, the border of which is indicated by a dotted line. N, neuron. Scale bar, 50 μm.

(C) A typical view of an overlaid astrocyte attaching itself to a neuron on a microisland. The astrocyte plasma membrane was labeled with EGFP. N, neuron; A, astrocyte. Scale bar, 50 μm.

(D) A series of time-lapse images of the same neuron and astrocyte shown in (C), showing astrocytic movement along the neurites. Scale bar, 50 μm.

http://www.neuron.org/cgi/content/full/41/3/405/DC1), suggesting the maturation of these presynaptic terminals. The astrocyte-dependent maturation of presynaptic terminals was examined in greater detail using the FM1-43 dye. FM1-43 labeling was performed by depolarizing the neuron for 90 s in a high-K^+ (90 mM KCl) buffer. Under these conditions, neurons co-cultured with astrocytes (n = 19 cells) for 2 days displayed three times the number of fluorescent puncta as isolated neurons (n = 12 cells) (Figure 2A). In addition, the fluorescence of the puncta of neurons in contact with astrocytes was roughly twice as intense as that seen in isolated neurons. Using identical observation conditions, the average fluorescence intensities of FM 1-43-labeled puncta in Control and Astrocyte Plus samples were 630 ± 130 (n = 303) and 1,280 ± 240 (n = 414), respectively. Destaining of FM dye-labeled puncta reflects calcium-dependent transmitter release (Ryan, 2001). Subsequent FM1-43 destaining, induced by depolarization stimulation, was more rapid and extensive in the puncta of neurons in contact with astrocytes (Figure 2B, bottom, Astrocyte Plus) than of isolated neurons (Figure 2B, top, Control). Puncta destaining was analyzed by the evaluation of two quantities. The first was the decrease in fluorescence of individual puncta 220 s after stimulation, expressed as a percentage of the initial levels. The statistical distribution of fluorescence decrease values, as recorded from 19 neurons in contact with astrocytes, gave a Gaussian-like curve peaking at 34.4 ± 9.8% (n = 414 puncta) (Figure 2C, black bars). By contrast, the distribution for 12 isolated neurons was broad, with a peak at 16.2 ± 9.9% (n = 303 puncta) (Figure 2C, gray bars). The other quantity measured was the rate of destaining, τ, which was shorter and more uniform in the 19 neurons co-cultured with astrocytes (14.3 ± 7.7 s, n = 414 puncta) than in the 12 control neurons (47.3 ± 59 s, n = 303 puncta) (Figure 2D). The higher destaining rate of the FM dyes may suggest that astrocyte contact changes neurotransmitter release properties as well as the number of release sites.

Effects of Astrocyte on Autaptic EPSC Amplitude

To examine effects of astrocyte contact on synaptic strength, autaptic EPSC amplitude was measured in neurons untreated (Control) or overlaid with astrocytes (Astrocyte Plus). Figure 3A shows typical responses to paired-pulse stimuli (50 ms interval). The amplitude of the EPSC was significantly enhanced by astrocyte contact. Similar results were obtained from other experiments using eight Control samples and eight Astrocyte Plus samples. Statistically, the astrocyte-dependent increase in the EPSC amplitude was about 5-fold (Control, 582 ±142 pA, n = 9; Astrocyte Plus, 2,522 ± 388 pA, n = 9, $p < 0.01$) (Figure 3B). There were no significant differences in the series resistance (Rs) of whole-cell recordings (Control, 16.0 ± 0.5 MΩ; Astrocyte Plus, 14.5 ± 0.8 MΩ), the amplitude of holding currents at −70 mV (Control, 125 ± 79 pA; Astrocyte Plus, 56 ± 16 pA), or the input resistance (Control, 484 ±107 MΩ; Astrocyte Plus, 410 ±84 MΩ) between the two groups (data not shown). Under these recording conditions, EPSCs failed to be observed only in two untreated neurons (Control). The paired-pulse modulation ratio (PPMR), defined as the relative amplitude of the second EPSC to the first EPSC, was examined. The statistical value was 0.73 ± 0.07 for Control and 0.74 ± 0.06 for Astrocyte Plus neurons (Figure 3C).

Subsequently, asynchronous excitatory postsynaptic currents (EPSCs) were recorded following stimuli (Figure 3D). Comparison of the amplitude histograms of the Control (n = 9) and Astrocyte Plus (n = 9) samples reveals that there was no difference (Kolomogorov-

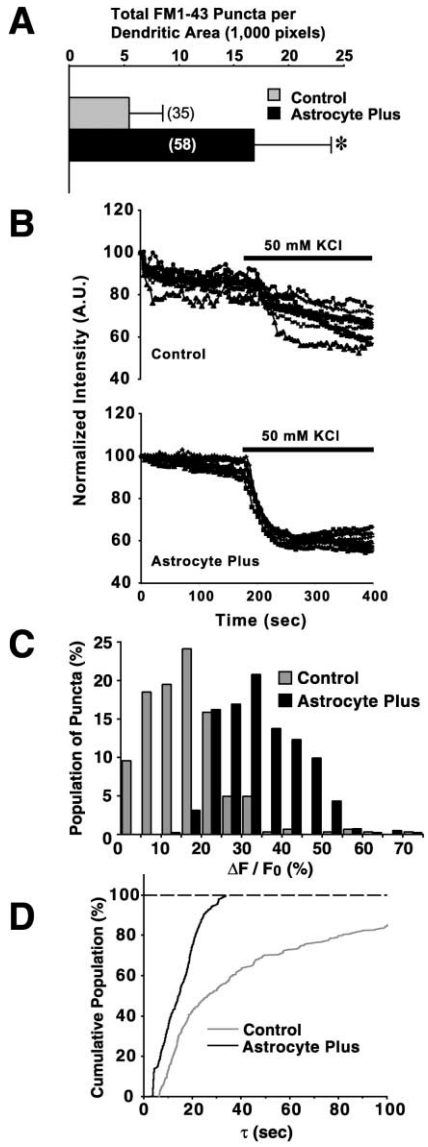

Figure 2. Increase in the Number and Activity of Presynaptic Release Sites following Astrocyte Overlay

(A) The total number of FM1-43-labeled puncta per dendritic area (Control, n = 35 dendrites of 11 neurons; Astrocyte Plus, n = 58 dendrites of 19 neurons). *t test, $p < 0.01$.

(B) Time courses of FM1-43-labeled puncta fluorescence intensities observed in a solitary neuron (top) and in a neuron overlaid with astrocytes (bottom) following stimulation with 50 mM KCl.

(C) The distribution of the percent decreases in fluorescence intensity of the puncta population from 12 solitary neurons (Control) and 19 neurons overlaid with astrocytes (Astrocyte Plus) 220 s after stimulation with 50 mM KCl. Statistical analysis was performed by the t test ($p < 0.01$).

(D) Cumulative population plot of the FM1-43 destaining rates of 12 solitary neurons (gray line) and 19 neurons overlaid with astrocytes (black line). Statistical analysis was performed by the t test ($p < 0.01$).

Smirnov test, $p > 0.1$) in the size of asynchronous EPSCs (Figure 3E). It is therefore unlikely that the sensitivity of AMPA receptors is altered by astrocyte contact. By contrast, the frequency of the asynchronous EPSC was significantly increased by contact with astrocytes (Figure 3F). The increase in frequency can be accounted for by enhanced efficacy of transmitter release at individual release sites, or by an increased number of functional synapses.

Global Facilitation of Synaptogenesis after Local Contact with Astrocytes

To examine synaptogenesis in cultured neurons, we focused on the formation of excitatory synapses through immunocytochemistry, using antibodies against PSD-95 and synaptotagmin I, markers for post- and presynaptic specialization, respectively (Südhof and Scheller, 2001; Sheng, 2001). Within 24 hr after the addition of astrocytes, the majority of neurons generated multiple puncta which stained positive for both PSD-95 and synaptotagmin I along their processes (Figure 4A, bottom, Astrocyte Plus). This result suggests that contact with astrocytes induces the formation of excitatory synapses (Figure 4B, black bar). Without astrocyte overlay, no colocalization of PSD-95 and synaptotagmin I was observed (Figures 4A, top and Figure 4B, gray bar).

As the colocalization of PSD-95/synaptotagmin I and FM-dye staining were observed over the entire neuron, while physical contact with astrocytes appeared to occur locally, we hypothesized that local astrocytic contact elicits global augmentation of excitatory synaptogenesis. To test this hypothesis, we examined whether synapse-formation signals could be detected in regions distal to sites of astrocyte contact. Two neurons on a single microisland were stained with FM4-64, and their immaturity was confirmed by the absence of staining along their processes (Figure 4C). An astrocyte was then overlaid onto the cells, and the movements of all three cells were visualized for 42 hr by time-lapse imaging. A cumulative image showing the footprint of the astrocyte on the neurons (Figure 4D) clearly distinguishes between regions touched and untouched by the astrocyte. Subsequent staining with FM4-64 exhibited uniformly high signal in all regions of the neurons (Figure 4E), regardless of whether they had come into contact with the astrocyte. Upon immunocytochemical staining, significant levels of both PSD-95 and synaptotagmin I were detected in a punctate pattern in regions distal to astrocyte contact (Figure 4E, bottom, two boxes).

PKC Activation Is Triggered by Astrocytic Contact

If global facilitation of synaptogenesis within a neuron results from local contact with astrocytes, the signaling molecules involved in the process remain unknown. To identify the signaling pathways triggered by astrocytic contact, we screened several candidate signaling molecules. Intracellular Ca^{2+} concentration ($[Ca^{2+}]_i$) was monitored using either fura-2 or cameleon (Miyawaki et al., 1997), a genetically encoded indicator for Ca^{2+}. No significant changes were detected after the addition of astrocytes (data not shown). Time-lapse images using Raichu-Ras (Mochizuki et al., 2001), an indicator of Ras activation, also yielded no changes in signal strength between control and astrocyte-containing cultures. Next we examined phosphorylation events using immunocytochemistry with antibodies specific for phosphorylated molecules. While the phosphorylation of MAPK/Erk-2, JAK/STAT, and src family proteins remained unchanged, a polyclonal antibody against phosphorylated myristoy-

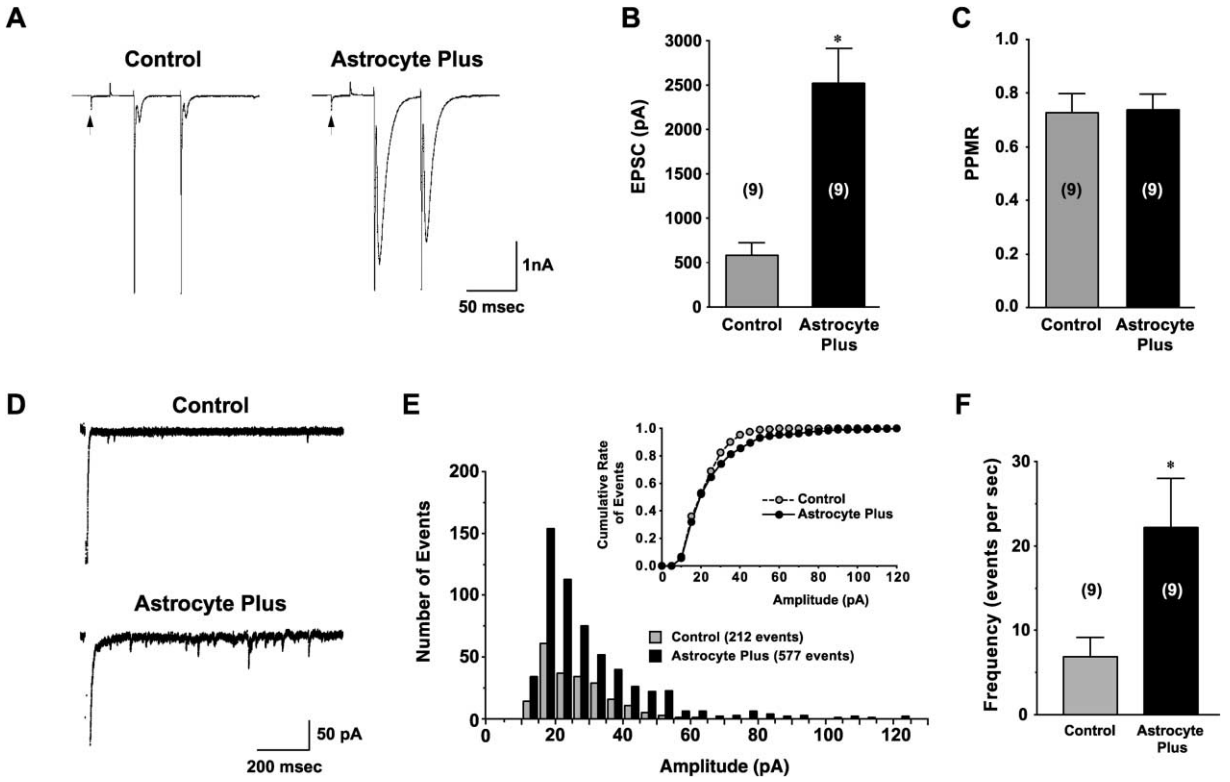

Figure 3. Autaptic EPSCs in Cultured Hippocampal Neurons

(A) Typical EPSCs evoked by paired-pulse stimuli (50 ms interval) in a neuron untreated (Control) or overlaid with an astrocyte (Astrocyte Plus). A hyperpolarizing pulse (5 mV) was applied at the beginning of each stimulation (indicated by an arrow) to measure series and input resistance.

(B) Amplitudes of the first evoked EPSCs in Control ($n = 9$) and Astrocyte Plus ($n = 9$) neurons. *t test, $p < 0.01$

(C) Paired-pulse modulation ratios (PPMRs) in Control ($n = 9$) and Astrocyte Plus ($n = 9$) neurons.

(D) A typical trace of asynchronous EPSCs recorded in a neuron untreated (Control) or overlaid with an astrocyte (Astrocyte Plus).

(E) Histograms of asynchronous EPSCs. Events were collected from four traces of each neuron (Control, $n = 9$; Astrocyte Plus, $n = 9$). Both groups show the same quantal size (17 pA), represented by the mode of distribution. (Inset) Cumulative amplitude distributions of the histograms.

(F) Frequency of asynchronous EPSCs in a neuron untreated (Control, $n = 9$) or overlaid with an astrocyte (Astrocyte Plus, $n = 9$). Statistical analysis was performed by ANOVA with the Bonferroni method ($p < 0.05$).

lated alanine-rich C kinase substrate (P-MARCKS) revealed differences in reactivity in neurons dependent on contact with astrocytes.

MARCKS is one of the predominant PKC substrates and is present in many cell types (Ohmori et al., 2000). Immunocytochemical examination of early phosphorylation of MARCKS (i.e., 40 min after contact with astrocytes) by PKC reproducibly detected P-MARCKS immunoreactivity (IR-P-MARCKS) in 50 neurons subjected to astrocyte adhesion (Figure 5A, Astrocyte Plus). IR-P-MARCKS was occasionally detected in isolated neurons (Figure 5A, Control), but only within filopodial structures. IR-P-MARCKS intensities recorded from neurons were normalized to control values (Figure 5A, right). Pretreatment of neuron/astrocyte complexes with 5 μM GF109203X, an inhibitor of PKC activity (Toullec et al., 1991), greatly reduced the IR-P-MARCKS signal (Figure 5A, Astrocyte Plus +GFX), indicating that PKC enzymes were primarily responsible for the observed MARCKS phosphorylation. While we used astrocytes prepared from the cerebral cortex in this study, astrocytes derived from the spinal cord were also overlaid to test astrocyte cell specificity. Interestingly, a spinal cord astrocyte significantly induced MARCKS phosphorylation but to a slightly lesser extent than seen with cortical astrocytes (Figure 5A, Spinal Cord Astrocyte Plus). Meningeal fibroblasts, however, did not produce increases in IR-P-MARCKS, except in filopodial structures (Figure 5A, Meningeal Fibroblast Plus). Importantly, MARCKS immunoreactivity localized uniformly within these cell samples, irrespective of the location of astrocyte contact (data not shown). Taken together, these results demonstrate that PKC signaling is activated uniformly throughout neurons following localized astrocytic contact.

Integrin Reception Occurs during Astrocytic Contact

Next, we sought to determine the surface molecules responsible for astrocyte/neuron communication. We found that an integrin blocker, echistatin, completely suppressed IR-P-MARCKS in neurons, while preserving signals in adjacent astrocytes (Figure 5A, Astrocyte Plus +Echistatin). Therefore, we examined the effect of pretreatment of cell samples with various cell-cell adhesion-blocking peptides on IR-P-MARCKS signal in

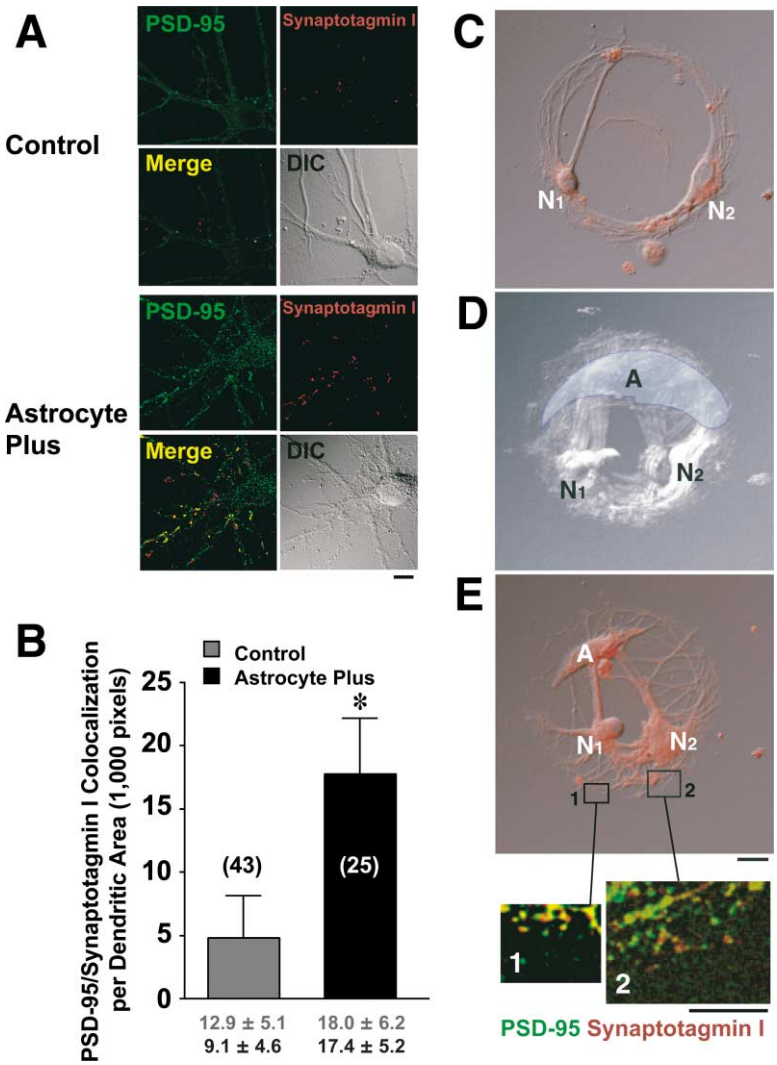

Figure 4. Enhanced Formation of Excitatory Synapses in Regions Distal to the Sites of Astrocytic Contact

(A) Fluorescence images showing immunoreactivity for PSD-95 (green) and synaptotagmin I (red) and colocalization of PSD-95/synaptotagmin I (Merge), together with confocal differential interference contrast (DIC) images of a solitary neuron (Control) and a neuron in contact with an astrocyte (Astrocyte Plus). Scale bar, 10 μm.

(B) PSD-95/synaptotagmin I colocalization in the dendrites of 15 isolated neurons (Control, n = 43) and ten neurons in contact with astrocytes (Astrocyte Plus, n = 25). *t test, $p < 0.01$.

(C) FM4-64 staining of two neurons (N1 and N2) on a microisland prior to astrocyte overlay.

(D) Cumulative image of an overlaid astrocyte and two neurons (N1 and N2) throughout the time-lapse imaging over 42 hr. The footprint of the astrocyte is shown in blue. A, astrocyte.

(E) FM-4-64 staining of N1, N2, and the overlaid astrocyte 42 hr after initial contact (top). Insets 1 and 2 depict the colocalization of PSD-95 (green) and synaptotagmin I (red) in the indicated areas.

Scale bars, 20 μm in (C)–(E) and 5 μm in boxes 1 and 2 of (E).

neurons 40 min after contact with astrocytes (Figure 5B). The RGDS peptide (100 μM), which blocks integrin interactions, completely abolished IR-P-MARCKS signals in a manner similar to echistatin. The YIGSR peptide (100 μM), an inhibitor of laminin, lowered the signal only slightly, while an inhibitor of neural cell adhesion molecule (NCAM), the KHIFSDDSSE peptide (1 mM) (Kam et al., 2002), had no effect on IR-P-MARCKS (Figure 5B, Astrocyte Plus +NCAM peptide). These results indicate that integrin receptors are primarily responsible for relaying signals from astrocytes to neurons. Echistatin selectively blocks integrin complexes containing either the β1 or β3 subunit (Pfaff et al., 1994). Indeed, we verified by immunocytochemistry that the neurons used in our experiments expressed significant levels of β1 subunit on their plasma membranes (Supplemental Figure S3A at http://www.neuron.org/cgi/content/full/41/3/405/DC1). The poor suppression of IR-P-MARCKS by the YIGSR peptide suggested that the laminin ligand is not effective to trigger PKC activation. In support of this conclusion, the treatment of isolated hippocampal neurons with mouse laminin (2 μg/ml in the medium) induced increased extension of their neurites, but did not induce either IR-P-MARCKS or enhanced synaptogenesis (results not shown).

Arachidonic Acid Release Links Integrin Reception to PKC Activation

Previous studies have shown that both integrin-β1-mediated adhesion of HeLa cells and the spreading of NIH-3T3 cells lead to PKC activation through phospholipase A_2 (PLA2)-mediated arachidonic acid release (Auer and Jacobson, 1995; Whitfield and Jacobson, 1999). In addition, the novel PKC isoform PKC-ε requires arachidonic acid to translocate from the cytosol to the plasma membrane (Shirai et al., 1998) and anchor onto actin fibers (Prekeris et al., 1996). By immunocytochemistry, we detected significant amounts of PKC-ε throughout the neurons used in our experiments (Supplemental Figure S3B at http://www.neuron.org/cgi/content/full/41/3/405/DC1). To test the involvement of arachidonic signaling, we examined the effects of lipid second messenger inhibitors on the phosphorylation of MARCKS. Both Mepacrine, a PLA2 inhibitor (10 μM), and E-6-(bromomethylene)tetrahydro-3-(1-naphthalenyl)-2H-pyran-2-one (HELSS) (1 μM), an inhibitor of calcium-independent PLA2 (iPLA2), greatly

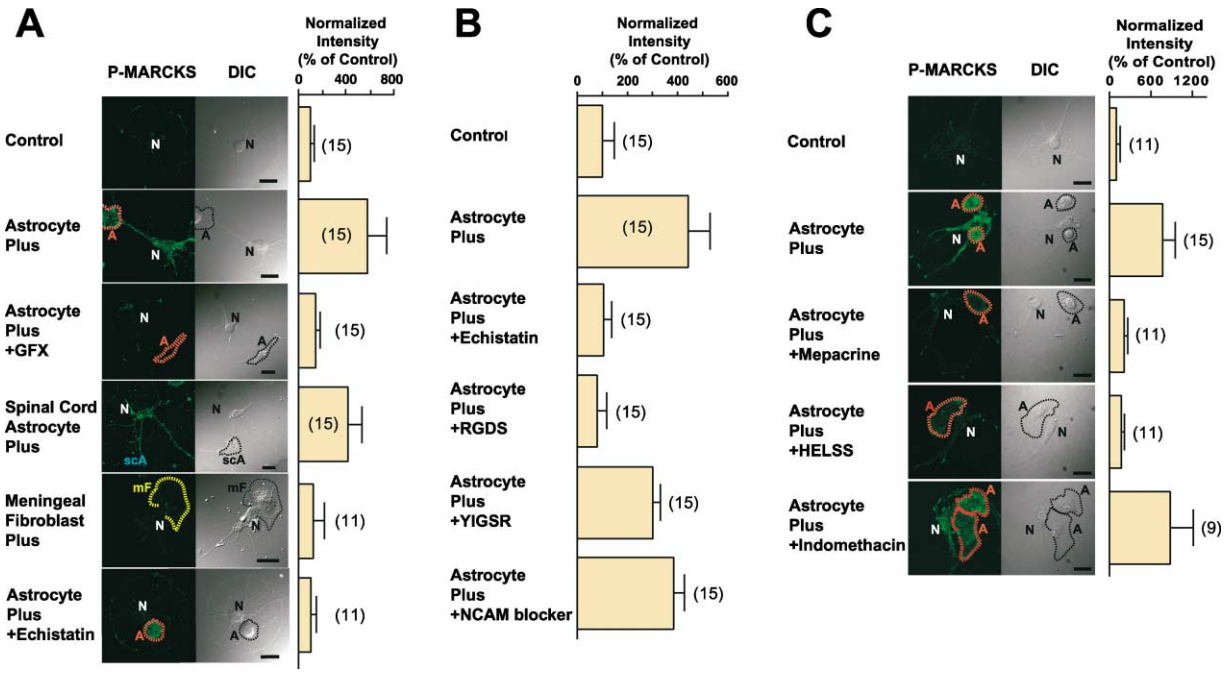

Figure 5. Phosphorylation of MARCKS in Neurons on Microislands 40 Minutes after Contact with Astrocytes

Fluorescence images demonstrating immunoreactivity for phosphorylated MARCKS (P-MARCKS) (A and C) with DIC images (A and C). Bar graphs summarize the quantitative analysis of immunoreactivity with the number of neurons assayed shown in parentheses (A–C).

(A) No astrocytes were added in the top picture (Control). Cells were fixed 40 min after initial contact with astrocytes (Astrocyte Plus; Astrocyte Plus + GFX; Astrocyte Plus + Echistatin), spinal cord astrocytes (Spinal Cord Astrocyte Plus), and meningeal fibroblasts (Meningeal Fibroblast Plus). Outlines of the overlaid cells are indicated by dotted lines. Where specified, 5 μM GF109203X was added to the medium (Astrocyte Plus + GFX). Scale bars in DIC images, 20 μm. N, neuron; A, astrocyte; scA, spinal cord astrocyte; mF, meningeal fibroblast.

(B) Bar graph showing effects of various peptides on MARCKS phosphorylation in neurons. Scale bars in DIC images, 20 μm.

(C) Fluorescence images, DIC images, and bar graphs showing the effects of inhibitors of lipid second messengers on the phosphorylation of MARCKS. Scale bars in DIC images, 20 μm. Statistical analysis was performed by ANOVA with the Bonferroni method ($p < 0.01$) (A–C).

reduced the IR-P-MARCKS signal in neurons that had been in contact with astrocytes (Figure 5C, Astrocyte Plus +Mepacrine and Astrocyte Plus +HELSS). In contrast, the cyclooxygenase inhibitor indomethacin (5 μM) had no effect on IR-P-MARCKS signals (Figure 5C, Astrocyte Plus +Indomethacin).

Time-Lapse Imaging of PKC Activation through MARCKS Translocation

MARCKS binds to the plasma membrane by inserting its hydrophobic myristate chain into the lipid bilayer, an interaction stabilized by the electrostatic interaction of the basic effector domain residues with the acidic membrane phospholipids (Arbuzova et al., 2002). Phosphorylation of MARCKS by PKC adds multiple negative charges to the basic cluster, reducing these electrostatic interactions; in many cell types, phosphorylation results in the translocation of MARCKS from the membrane to the cytoplasm. To observe PKC activation in live neurons, we examined the localization of MARCKS using a Cy3.5-labeled monoclonal antibody (αMARCKS-Cy3.5), which binds the C terminus of the protein. This antibody was microinjected into isolated neurons cultured on microislands, and the signal was monitored before and after astrocyte overlay (Supplemental Figure S4B). Following injection, αMARCKS-Cy3.5 fluorescence was initially localized to the neuron plasma membrane. The distribution of αMARCKS-Cy3.5 signal was estimated by measuring the relative fluorescence intensity in a region of the cytosol versus the plasma membrane. Ten to 15 min after contact between a major dendritic process and an astrocyte, translocation of the fluorescent signal to the cytosol from the plasma membrane was observed not only in the astrocyte-contacting process but also in an independent primary process (Supplemental Figure S4B at http://www.neuron.org/cgi/content/full/41/3/405/DC1). The cytosolic distribution was sustained throughout the 3 hr observation period. In contrast, αMARCKS-Cy3.5 fluorescence was always localized to the plasma membrane in control neurons without astrocyte overlay (Supplemental Figure S4A).

Long-Lasting PKC Activation Caused by Astrocytic Contact

Astrocyte-dependent IR-P-MARCKS remained at high intensity throughout the later stages of the experiments (2 days following the addition of astrocytes) (Figure 6, Astrocyte Plus). After astrocyte contact, a strong IR-P-MARCKS signal was detected throughout the entire neuron; weak and diffuse IR-P-MARCKS was observed in the peripheral region of the astrocyte. Immunocytochemistry using anti-MARCKS antibodies confirmed that the total amount of MARCKS protein did not change

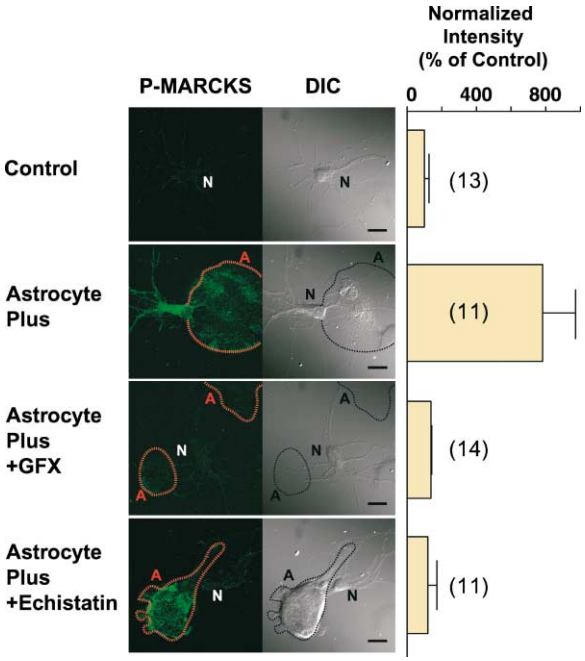

Figure 6. Phosphorylation of MARCKS in Neurons on Microislands 2 Days after Contact with Astrocytes

Fluorescence images showing immunoreactivity for phosphorylated MARCKS (P-MARCKS), DIC images, and bar graphs summarizing the quantitative analysis of immunoreactivity. The number of assayed neurons is indicated in parentheses. P-MARCKS was labeled in green. Neurons overlaid with astrocytes were fixed for immunocytochemistry 2 days after overlay. Astrocytes are outlined by dotted lines. GF109203X (5 μM) and echistatin (0.5 μM) were added to medium where indicated. Scale bars, 20 μm. Statistical analysis was performed by ANOVA with the Bonferroni method ($p < 0.01$).

during the 2 day incubation with astrocytes (data not shown). Chronic treatment of cell samples with 5 μM GF109203X abolished the MARCKS signal in both neurons and astrocytes (Figure 6, Astrocyte Plus +GFX). Significantly, the disintegrin peptide echistatin (0.5 μM) suppressed IR-P-MARCKS in the neuron, but not in the adjacent astrocyte (Figure 6, Astrocyte Plus +Echistatin). Such differential suppression of PKC activation by this reagent indicates that integrin molecules are critical in the maintenance of neuron/astrocyte contacts as well as the activation of PKC signaling. It should be noted that the astrocyte did physically contact the neuron (Figure 6, Astrocyte Plus +Echistatin); although the astrocyte shrank, it made contact with several neuronal processes beforehand. The requirement of integrin engagement may also rule out the possibility that PKC signaling was triggered by astrocyte-derived diffusible factors. Although the magnitude of IR-P-MARCKS signal is determined by the balance of PKC and phosphatase activities on MARCKS, efficient detection of IR-P-MARCKS at late stages suggests the requirement of sustained activation of PKC for synaptogenesis (see below).

PKC Signaling and Synaptogenesis

As global PKC activation and facilitation of synaptogenesis result from local contact with astrocytes, we explored the extent to which PKC signaling is required for excitatory synaptogenesis. We examined the immunolocalization of AMPA-type glutamate receptor 1 (GluR1), a marker for active postsynaptic membrane, and synaptophysin, a presynaptic marker. The colocalization of these molecules strongly suggests the presence of functional excitatory synapses. Astrocytic contact greatly increased the number of puncta containing both GluR1 and synaptophysin (Figure 7, Astrocyte Plus). In contrast to a previous report (Dijkstra et al., 1999), however, astrocyte contact did not augment the branching of processes. Conversely, laminin induced significant neurite extension of isolated neurons without causing PKC activation or enhanced synaptogenesis (data not shown). These findings indicate that enhancement of synaptogenesis is a separate process altogether from neurite extension.

To test the requirement of PKC activation via integrin receptor engagement for astrocyte-dependent facilitation of synaptogenesis, we blocked integrin reception or PKC activity pharmacologically. Astrocyte-associated neuronal maturation was suppressed by pretreatment with either echistatin (Figure 7, Astrocyte Plus +Echistatin) or GF109203X (Figure 7, Astrocyte Plus +GFX). The application of GF109203X led to a clustering of synaptophysin immunoreactivity within the cell soma. Although the sustained activation of PKC, as caused by astrocyte contact, cannot be precisely reproduced by pharmacological means, we treated isolated neurons on microislands with 1 μM phorbol 12,13-didecanoate (PDD), a PKC activator, for 2 days with a 1 day interval incubation in normal medium. These culture conditions gave rise to a significant number of puncta immunostained for both GluR1 and synaptophysin (Figure 7, PDD), demonstrating that PKC activation is sufficient for excitatory synaptogenesis of neurons.

Discussion

Although it is widely accepted that astrocytes participate actively in synaptogenesis of purified neurons in vitro, the molecular mechanism by which these cells act has not been fully understood. A fundamental question remains as to whether the responsible factors are diffusible or membrane bound. Growing evidence suggests that astrocytes function through a trophic mechanism. Pfrieger and Barres (1997) reported that the synaptic efficacy of postnatal rat retinal ganglion cells (RGCs) was enhanced by co-culture with glial cells. Barres and colleagues subsequently observed that the number of functional RGC synapses also increased in the presence of astrocyte-conditioned medium (Ullian et al., 2001). The diffusible factor responsible for these effects has recently been identified by Pfrieger and colleagues as cholesterol in complex with apolipoprotein E-containing lipoproteins (Mauch et al., 2001). However, the identification of this factor does not preclude the contribution of membrane-bound factors in the enhancement of synaptic efficacy, and this possibility has not been explored extensively. While astrocytes appear to make local contact with neurons, it has not been shown whether the effects on excitatory synaptogenesis are localized to the contact sites or propagated throughout the neuron.

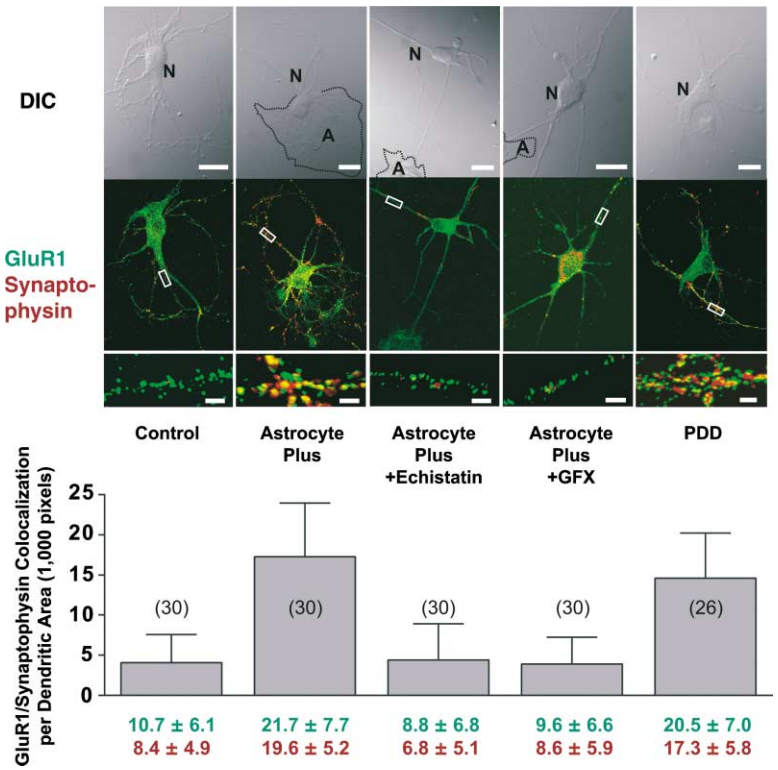

Figure 7. Maturation of Functional Excitatory Synapses in Neurons following Contact with Astrocytes

Fluorescence images showing immunoreactivity for GluR1 (green) and synaptophysin (red), DIC images, and bar graphs summarizing the quantitative analysis of GluR1/synaptophysin colocalization. Parentheses indicate the number of assayed dendrites on ten neurons examined. Except for Control and PDD-treated neurons, cells were fixed for immunocytochemistry 2 days after astrocyte contact. N, neuron; A, astrocyte. Astrocytes are outlined by dotted lines. Echistatin (0.5 μM) and GF109203X (5 μM) were added to the medium where noted. Phorbol 12,13-didecanoate (PDD) (1 μM) was added to the medium on day 1 and day 3 (PDD). The lower fluorescence images represent higher-magnification views of the outlined boxes. Scale bars, 20 μm in DIC images and 2 μm in expanded fluorescence images. Statistical analysis was performed by ANOVA with the Bonferroni method ($p < 0.01$).

In addition, because astrocytes move and change shape dynamically while in contact with neurons, this question can only be properly addressed by monitoring contact sites over time, as with time-lapse imaging.

In this study, we tracked mature astrocytes during their contact with isolated hippocampal neurons, which had been grown on spots of permissive substrate in the presence of astrocyte-conditioned medium. The formation of excitatory synapses was examined by the efficiency of both FM dye staining and destaining (Figures 2 and 4), and colocalization of immunostaining for PSD-95 and synaptotagmin I (Figure 4B) or GluR1 and synaptophysin (Figure 7). The colocalization signals were increased several-fold, which was consistent with the observed 5-fold enhancement of the EPSC amplitude (Figure 3). Our study investigating the spatial and temporal patterns of astrocytic contact and synapse formation revealed that local contact with astrocytes promotes global excitatory synaptogenesis in neurons (Figures 4D and 4E). It is difficult, however, to separate the effects of direct contact from the effects of short-range diffusible factors, opening the possibility that astrocytic contact provides the permissive conditions for the action of diffusible factors. Regardless of the involvement of diffusible factors, here we present evidence for the requirement of membrane-bound factors, demonstrating pharmacologically the requirement for integrin receptor binding in astrocyte-dependent synaptogenesis.

In contrast to our results, previous reports (Ullian et al., 2001; Mauch et al., 2001) concluded that astrocyte-derived diffusible factors were able to significantly facilitate synaptogenesis. This apparent discrepancy may be explained by differences between the hippocampal neurons we used and the retinal ganglion cells (RGCs) used by other groups, in that the two cell types may demonstrate differential dependence upon astrocyte-derived diffusible versus membrane-bound factors. Alternatively, it is possible that the two factors work at different levels of synaptogenesis. Although synaptogenesis was not facilitated in isolated hippocampal neurons following the application of cholesterol (10 μg/ml) (Supplemental Figure S5 at http://www.neuron.org/cgi/content/full/41/3/405/DC1), which exerted a significant effect on RGCs (Mauch et al., 2001), cholesterol might have been present at saturating concentrations under the conditions in the present study. In fact, Hering et al. (2003) reported that depletion of cholesterol/sphingolipid led to a gradual loss of synapses in cultured hippocampal neurons. Here, we claim that full facilitation of synaptogenesis requires astrocyte contact in addition to astrocyte-derived diffusible factors.

Our study can also be compared with data from Rao et al. (2000), in which high-density synapses developed on isolated hippocampal neurons growing without glial contact. In this study, however, they detected clustering of synaptic elements only after 16 days in culture in the presence of high concentrations of diffusible factors from astrocytes. As our system used over a hundred times more astrocytes per neuron than this study, it is likely that the concentration of astrocyte-derived factors was saturated in our cultures. In fact, colocalization of GluR1/synaptophysin increased slightly in our control cultures, but only after 18 days in culture (Supplemental Figure S5 at http://www.neuron.org/cgi/content/full/41/3/405/DC1). However, astrocytic overlay at early stages (8–9 days in vitro, DIV 8–9) for 2–3 days brought about several fold higher density of nascent synapses (Supplemental Figure S5) than isolated older neurons. These results indicate that astrocyte contact acts on isolated hippocampal neurons more rapidly and to a greater extent than astrocyte-derived diffusible factors.

We have found reproducible evidence of global activation of PKC signaling within individual neurons after local contact with astrocytes. Immunostaining for phosphorylated MARCKS, a PKC substrate present in many cell types (Albert et al., 1986), was observed in neurons 40 min and 2 days following initial astrocyte contact (Figures 5 and 6, respectively). Immediate and long-lasting PKC activation was observed after neuron-astrocyte contact by monitoring neuronal redistribution of MARCKS, as phosphorylation of MARCKS by PKC also results in the translocation of MARCKS from the plasma membrane to the cytoplasm. Although the binding of a Ca^{2+}-CaM complex to the basic effector domain of MARCKS might also induce a similar translocation, this mechanism is unlikely to function in astrocyte-induced MARCKS redistribution for two reasons. First, no changes in cytosolic Ca^{2+} concentrations were detected after astrocytic contact (data not shown). Second, there have not been any reports observing in situ complex formation between MARCKS and Ca^{2+}-CaM. In addition, a direct interaction between MARCKS and Ca^{2+}-CaM was detected only when PKC activity was pharmacologically blocked in FRET experiments using a chimeric cyan fluorescent protein-CaM (CFP-CaM) and a MARCKS-yellow fluorescent protein (MARCKS-YFP) (Sawano et al., 2002). We therefore conclude that, under physiological conditions, translocation of MARCKS is strictly an indicator of PKC activation.

As both MARCKS phosphorylation and synapse maturation were observed globally throughout the neuron, the observed PKC activation appeared to be responsible for the facilitation of excitatory synaptogenesis. Treatment of neurons with GF109203X, a PKC inhibitor, markedly diminished staining for phosphorylated MARCKS while also impairing synaptogenesis. Another well-known PKC substrate, adducin (Benett et al., 1988), can be used to observe global PKC activation in neurons after local contact with astrocytes (Supplemental Figure S6 at http://www.neuron.org/cgi/content/full/41/3/405/DC1). Since MARCKS and adducin are associated with F-actin fibers and spectrin, respectively, it is likely that cytoskeletal changes, such as actin-based spinogenesis, may be important for the enhancement of synaptogenesis (Matus, 2000) (Figure 8). The identification of other PKC substrates phosphorylated upon neuronal contact with astrocytes will help to elucidate the molecular mechanisms governing synaptic maturation. Recently, several reports have detailed the involvement of PKC signaling in synaptic function. Fong et al. (2002) found that selective activation of PKC with phorbol esters (TPA) induced rapid dispersal of NMDA receptors and the accumulation of CaMKII in postsynaptic sites within one hour of treatment. Daw et al. (2000) reported that treatment with TPA also induced the insertion of AMPA receptors into the plasma membrane. Such examples of postsynaptic remodeling following TPA administration have been studied during a period of one or two hours, while our present study discusses the regulation of PKC activation over longer, more physiological time frames. Figure 8 illustrates the overall signaling schematic described herein, detailing the progression from local contact between neuron and astrocyte to the global facilitation of synaptogenesis. Arachidonic acid or PKC(ε) enzymes may also contribute to the signal propagation as diffusible intracellular messengers.

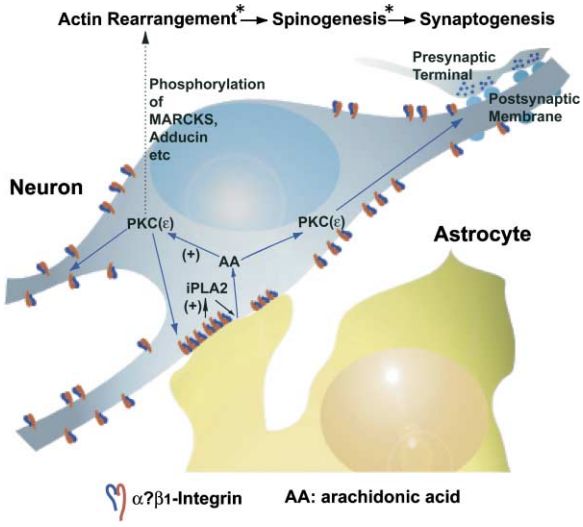

Figure 8. Schematic of the Intracellular Signaling Cascade Progressing from Local Astrocyte Contact to the Global Facilitation of Synaptogenesis

*Hypothetical events.

Adult neurogenesis occurs in two regions of the adult brain: the subventricular zone (SVZ) and the hippocampal subgranular zone. Recently, Song et al. (2002a, 2002b) demonstrated that mature hippocampal astrocytes regulate neurogenesis by instructing stem cells to adopt a neuronal fate. These studies detail a marked increase in neuronal production from adult stem cells plated on a feeder layer of astrocytes. As highly efficient neurogenesis occurred upon the plating of adult stem cells on either coated substances conditioned by primary astrocytes or directly on light-fixed astrocytes, the authors concluded that both diffusible and membrane-bound astrocyte-produced factors could promote neurogenesis. In another study, Lim and Alvarez-Buylla (1999) found that neurogenesis in adult-derived SVZ cells was supported by astrocyte monolayers, but not by astrocyte-conditioned medium. They consequently concluded that direct cell contact between SVZ precursors and live astrocytes was required for neurogenesis. Our immunohistochemical experiments performed using adult rat brain tissue demonstrated that immature neurons in the hippocampal subgranular zone, which experience a high degree of astrocyte contact, stained more positively for PKC activation than mature neurons in the granular cell layer (data not shown). Although there may be differences between the maturation of embryonic neurons and neurogenesis of adult neural stem cells, PKC signaling triggered by local cell-cell contact may be a general mechanism by which astrocytes regulate neuronal development.

Experimental Procedures

Cell Cultures

Neurons were prepared from Wistar rat fetuses (embryonic day 18–19) and plated on microislands as described previously (Goslin et al., 1998; Bekkers and Stevens, 1991). Microislands were created by spraying a solution of 2 mg/ml poly-L-lysine and 0.05 mg/ml

collagen onto a coverslip coated with 0.2% agarose. Astrocytes were prepared from 18-day-old rat embryo cerebral cortices (Hama et al., 1997), and maintained in DMEM containing 20% fetal bovine serum for 12–14 days before use. Astrocytes (DIV 12–14) were used to generate a feeder zone on the coverslip periphery (not coated with agarose), or overlaid onto neurons at DIV 8–9. In our experiments, a typical culture dish contained approximately 500,000 astrocytes at the rim, with approximately 20 isolated neurons grown on microislands at the center. The ratio of astrocytes to neurons was roughly 25,000, much higher than that achieved by Goslin et al. (1998) (70–230) for low-density culture of hippocampal neurons with confronting astrocytes. Spinal cord astrocytes and meningeal fibroblasts were prepared from rat fetuses (embryonic day 18). Basal Medium was prepared using phenol red-free MEM (Sigma) plus 1 mM sodium pyruvate, 3 mM glucose, 2 mM L-glutamine, 10 mM $MgCl_2$, 0.1% bovine serum albumin, and 15 mM HEPES (pH 7.2). Dissociated hippocampal neurons were suspended in Basal Medium containing N2 supplement (Gibco) and 10% horse serum, and plated onto microislands. Cell samples were kept in the same medium for 1 day. The medium was subsequently changed to Basal Medium containing N2 supplement, B27 supplement (Gibco), and 0.5% horse serum, which was used to keep the neurons on microislands while astrocyte-overlay experiments were conducted. GF109203X (Calbiochem) was added at a final concentration of 5 μM. Echistatin (Sigma) was added at a final concentration of 0.5 μM. At this concentration, we did not detect any effect on neurite growth or substratum attachment of the neurons.

Gene Construction and Transfection

Lyn-GFP was created by adding a sequence encoding the 22 N-terminal amino acids of the Lyn nonreceptor tyrosine kinase to the 5′ end of the cDNA for EGFP (enhanced GFP, Clontech) (Sawano et al., 2002). This chimeric protein is anchored to the plasma membrane through palmitate and myristate groups. Mature astrocytes were transfected with the cDNA encoding Lyn-GFP using Effectene (Qiagen).

Electrophysiology

Autaptic EPSCs were recorded in the whole-cell patch-clamp mode, low-pass-filtered at 3 kHz, and digitally sampled at 20 kHz using a patch-clamp amplifier (EPC-7, List Electronics, Darmstadt, Germany) (Yamaguchi et al., 2002). The bath solution consisted of 137 mM NaCl, 4 mM KCl, 2 mM $CaCl_2$, 1 mM $MgCl_2$, 17 mM glucose, and 10 mM HEPES-NaOH (pH 7.4). Picrotoxin (50 μM) and DL-AP5 (50 μM) were added during recording. The intrapipette solution consisted of 129 mM K-gluconate, 30 mM KCl, 2 mM $MgCl_2$, 1mM EGTA, 0.25 mM $CaCl_2$, 3 mM Na_2ATP, 0.3 mM GTP, and 5 mM HEPES (pH 7.2). Patch electrodes had resistances of 3-5 MΩ. Neurons were voltage clamped at -70 mV. A 1-ms voltage step to $+100$ mV was applied to evoke an autaptic EPSC. Five to ten EPSCs were sampled per cell. A paired-pulse stimulus with an interval of 50 ms was applied every 20 s. Series resistance compensation was not used. Asynchronous EPSCs were measured over a period of 0.9 s after an evoked EPSC, using the MINI ANALYSIS program (Jaejin Software, Leonia, NJ). All experiments were performed at room temperature (25–27°C). Most salts and chemicals used were obtained from Wako Biochemicals (Osaka, Japan). EGTA and Hepes were obtained from Dojindo laboratories (Kumamoto, Japan), K-gluconate, and picrotoxin were obtained from Sigma, and DL-AP5 was from Tocris.

Microinjection

A murine monoclonal antibody against MARCKS (αMARCKS, Upstate Biotechnology) was labeled with Cy3.5 reactive dye (Amersham Biotech). 2–10 pg labeled antibody (αMARCKS-Cy3.5) was injected into a single neuron using a glass capillary and FemtoJet (Eppendorf).

FM-Dye Staining and Destaining

Active presynaptic terminals were stained with 15 μM FM4-64 (Molecular Probes) or FM1-43 (Molecular Probes) as described (Ryan et al., 1993). Dye uptake was induced by depolarization for 90 s with 50 mM KCl. Cells were rinsed five times, then used for experiments after a 20 min incubation. Destaining experiments using FM1-43 were performed according to methods described previously (Ryan et al., 1993). The time constants of FM1-43 destaining were obtained by fitting destaining curves to single exponential decays (Chi et al., 2001). To minimize nonspecific staining, cells were rinsed with γ-cyclodextrin (2 mM) after loading with FM1-43 dye. Also, ROIs (regions of interest) for counting FM 1-43 dye-labeled puncta were placed over the processes free of overlaying astrocytes. Labeled synaptic puncta within 25–30 randomly selected regions within each neuron were analyzed using MetaFluor 4.5 software (Universal Imaging, Media, PA).

Immunocytochemistry

Cultured cells were immunostained as described previously (Tanaka et al., 2000; Yamamoto et al., 1998). Primary antibodies were used at the following dilutions: PSD-95, 1:400 (mouse, Upstate Biotechnology); synaptotagmin I, 1:250 (rabbit, Calbiochem); GluR1, 1:300 (rabbit, Upstate Biotechnology); synaptophysin, 1:400 (mouse, Sigma); and phosphorylated MARCKS, 1:100 (rabbit, TransGenic, Kumamoto, Japan). Appropriate secondary antibodies conjugated to Alexa Fluors 488 or 546 (Molecular Probes) were used at a dilution of 1:1000.

Microscopy

Image acquisition was performed using an Olympus FluoView 500 confocal microscope system equipped with an inverted microscope (IX80). All live and immunocytochemical images were collected with an Olympus 60X oil-immersion objective with numerical aperture 1.4. The 488 nm (argon) and 543 nm (He/Ne) laser lines were used for image acquisition. Colocalization of PSD-95 (green)/synaptotagmin I (red) or GluR1 (green)/synaptophysin (red) was quantified using Image Pro Plus 4.5.1 software (Media Cybernetics, Georgia, MD). Green and red images were merged and colocalized signals were automatically counted over each microisland. The theoretical analog focal resolution limit for the apparatus was calculated as $\sim$0.2 μm. For a pixel number set at 1,024 $\times$ 1,024, the pixel resolution was 0.25 μm. With a reduced iris aperture, our experiments utilized a z-resolution limit of $\sim$0.5 μm in our experiments. As the size of a dendritic spine is greater than 1 μm, our confocal system should be able to resolve adjacent synapses sufficiently (Lissin et al., 1998; Hohnke et al., 2000). To avoid cross-detection of green and red signals, images were sequentially acquired at 488 and 543 nm. The overall intensity of IR-P-MARCKS in each neuron was quantified in at least 3 ROIs (10 $\times$ 10 pixels), free of astrocyte-derived signals. Statistical analysis used Image Pro Plus 4.5.1 software. A CO_2 chamber (IBC, Olympus) was used for time-lapse imaging. An inverted microscope (IX70) was linked to a MicroMAX CCD camera (Roper Scientific) for FM1-43 destaining and MARCKS translocation experiments.

Acknowledgments

The authors would like to thank Yuichi Watanabe and Dr. Hideaki Mizuno for technical assistance; and Dr. Hideyuki Yamamoto, Dr. Naoaki Saito, and Dr. Masao Ito for valuable advice. This work was partly supported by grants from CREST of JST (Japan Science and Technology), the Japanese Ministry of Education, Science and Technology, and HFSP (Human Frontier Science Program).

Received: May 7, 2003
Revised: December 2, 2003
Accepted: December 29, 2003
Published: February 4, 2004

References

Albert, K.A., Walaas, S.I., Wang, J.K., and Greengard, P. (1986). Widespread occurrence of “87 kDa”, a major specific substrate for protein kinase C. Proc. Natl. Acad. Sci. USA *84*, 2822–2826.

Arbuzova, A., Schmitz, A.A.P., and Vergeres, G. (2002). Cross-talk unfolded: MARCKS proteins. Biochem. J. *362*, 1–12.

Auer, K.L., and Jacobson, B.S. (1995). Beta1 integrins signal lipid second messengers required during cell adhesion. Mol. Biol. Cell *6*, 1305–1313.

Bekkers, J.M., and Stevens, C.F. (1991). Excitatory and inhibitory autaptic currents in isolated hippocampal neurons maintained in cell culture. Proc. Natl. Acad. Sci. USA *88*, 7834–7838.

Benett, V., Gardner, K., and Steiner, J.P. (1988). Brain adducin: a protein kinase C substrate that may mediate site-directed assembly at the spectrin-actin junction. J. Biol. Chem. *263*, 5860–5869.

Chi, P., Greengard, P., and Ryan, T.A. (2001). Synapsin dispersion and reclustering during synaptic activity. Nat. Neurosci. *4*, 1187–1193.

Daw, M.I., Chittajallu, R., Bortolotto, Z.A., Dev, K.K., Duprat, F., Henley, J.M., Collingridge, G.L., and Issac, J.T.R. (2000). PDZ proteins interacting with C-terminal GluR2/3 are involved in a PKC-dependent regulation of AMPA receptors at hippocampal synapses. Neuron *28*, 873–886.

Dijkstra, S., Bär, P.R., Gispen, W.H., and Joosten, E.A.J. (1999). Selective stimulation of dendrite outgrowth from identified corticospinal neurons by homotopic astrocytes. Neuroscience *92*, 1331–1342.

Fong, D.K., Rao, A., Crump, F.T., and Craig, A.M. (2002). Rapid synaptic remodeling by protein kinase C: reciprocal translocation of NMDA receptors and calcium/calmodulin-dependent kinase II. J. Neurosci. *22*, 2153–2164.

Furuya, S., Tabata, T., Mitoma, J., Yamada, K., Yamasaki, M., Makino, A., Yamamoto, T., Watanabe, M., Kano, M., and Hirabayashi, Y. (2000). L-serine and glycine serve as major astroglia-derived trophic factors for cerebellar purkinje neurons. Proc. Natl. Acad. Sci. USA *97*, 11528–11533.

Goslin, K., Asmussen, H., and Banker, G. (1998). Rat hippocampal neurons in low-density culture. In Culturing Nerve Cells, G. Banker and K. Goslin, eds. (Cambridge, MA: MIT Press), pp. 339–370.

Hama, H., Kasuya, Y., Sakurai, T., Yamada, G., Suzuki, N., Masaki, T., and Goto, K. (1997). Role of endothelin-1 in astrocyte responses after acute brain damage. J. Neurosci. Res. *47*, 590–602.

Haydon, P.G. (2001). Glia: listening and talking. Nat. Rev. Neurosci. *2*, 185–193.

Hering, H., Lin, C.-C., and Sheng, M. (2003). Lipid rafts in the maintenance of synapses, dendritic spines, and surface AMPA receptor stability. J. Neurosci. *23*, 3262–3271.

Hohnke, C.D., Oray, S., and Sur, M. (2000). Activity-dependent patterning of retinogeniculate axons proceeds with a constant contribution from AMPA and NMDA receptors. J. Neurosci. *20*, 8051–8060.

Kam, L., Shain, W., Turner, J.N., and Bizios, R. (2002). Selective adhesion of astrocytes to surfaces modified with immobilized peptides. Biomaterials *23*, 511–515.

Lim, D.A., and Alvarez-Buylla, A. (1999). Interaction between astrocytes and adult subventricular zone precursors stimulates neurogenesis. Proc. Natl. Acad. Sci. USA *96*, 7526–7531.

Lissin, D.V., Gomperts, S.N., Carroll, R.C., Christine, C.W., Kalman, D., Kitamura, M., Hardy, S., Nicoll, R.A., Malenka, R.C., and Zastrow, M. (1998). Activity differentially regulates the surface expression of synaptic AMPA and NMDA glutamate receptors. Proc. Natl. Acad. Sci. USA *95*, 7097–7102.

Matus, A. (2000). Actin-based plasticity in dendric spines. Science *290*, 754–758.

Mauch, D.H., Nägler, K., Schumacher, S., Göritz, C., Müller, E.-V., Otto, A., and Pfrieger, F.W. (2001). CNS synaptogenesis promoter by glia-derived cholesterol Science *294*, 1354–1357.

Miyawaki, A., Llopis, J., Heim, R., McCaffery, J.M., Adams, J.A., Ikura, M., and Tsien, R. (1997). Fluorescent indicators for Ca^{2+} based on green fluorescent proteins and calmodulin. Nature *388*, 882–887.

Mochizuki, N., Yamashita, S., Kurokawa, K., Ohba, Y., Nagai, T., Miyawaki, A., and Matsuda, M. (2001). Spatio-temporal images of growth-factor-induced activation of Ras and Rap1. Nature *411*, 1065–1068.

Ohmori, S., Sakai, N., Shirai, Y., Yamamoto, H., Miyamoto, E., Shimizu, N., and Saito, N. (2000). Importance of protein kinase C targeting for the phosphorylation of its substrate, myristoylated alanine-rich C-kinase substrate. J. Biol. Chem. *275*, 26449–26457.

Pfaff, M., McLane, M.A., Beviblia, L., Niewiarowski, S., and Timpl, R. (1994). Comparison of disintegrins with limited variation in the RGD loop in their binding to purified integrins alpha IIb beta *3*, alpha V beta 3 and alpha 5 beta 1 and in cell adhesion inhibition. Cell Adhes. Commun. *2*, 491–501.

Pfrieger, F.W., and Barres, B.A. (1997). Synaptic efficacy enhanced by glial cells *in vitro*. Science *277*, 1684–1687.

Prekeris, R., Mayhew, M.W., Cooper, J.B., and Terrian, D.M. (1996). Identification and localization of an actin-binding motif that is unique to the epsilon isoform of protein kinase C and participates in the regulation of synaptic function. J. Cell Biol. *132*, 77–90.

Rao, A., Cha, E.M., and Craig, A.M. (2000). Mismatched appositions of presynaptic and postsynaptic components in isolated hippocampal neurons. J. Neurosci. *20*, 8344–8353.

Ryan, T.A. (2001). Presynaptic imaging techniques. Curr. Opin. Neurobiol. *11*, 544–549.

Ryan, A.T., Reuter, H., Wendland, B., Schweizer, F.E., Tsien, R.T., and Smith, S.J. (1993). The kinetics of synaptic vesicle recycling measured at single presynaptic boutons. Neuron *11*, 713–724.

Sawano, A., Hama, H., Saito, N., and Miyawaki, A. (2002). Multicolor imaging of Ca^{2+} and protein kinase C signals using novel epifluorescence microscopy. Biophys. J. *82*, 1076–1085.

Sheng, M.H.T. (2001). In Synapses, W.M. Cowan, T.C. Südhof, and C.F. Stevens, eds. (Baltimore, MD: The Johns Hopkins University Press), pp. 315–355.

Shirai, Y., Kashiwagi, K., Yagi, K., Sakai, N., and Saito, N. (1998). Distinct effects of fatty acids on translocation of γ-and ϵ-subspecies of protein kinase C. J. Cell Biol. *143*, 511–521.

Song, H., Stevens, C.F., and Gage, F.H. (2002a). Astroglia induce neurogenesis from adult neural stem cells. Nature *417*, 39–44.

Song, H., Stevens, C.F., and Gage, F.H. (2002b). Neural stem cells from adult hippocampus develop essential properties of functional CNS neurons. Nat. Neurosci. *5*, 438–445.

Südhof, T.C., and Scheller, R.H. (2001). In Synapses, W.M. Cowan, T.C. Südhof, and C.F. Stevens, eds. (Baltimore, MD: The Johns Hopkins University Press), pp. 177–215.

Tanaka, H., Shan, W., Phillips, G.R., Arndt, K., Bozdagi, O., Shapiro, L., Huntley, G.W., Benson, D.L., and Colman, D.R. (2000). Molecular modification of N-cadherin in response to synaptic activity. Neuron *25*, 93–107.

Toullec, D., Pianetti, P., Coste, H., Bellevergue, P., Grand-Perret, T., Ajakane, M., Baudet, V., Boissin, P., Boursier, E., Loriolle, F., et al. (1991). The bisindoylmaleimide GF 109203X is a potent and selective inhibitor of protein kinase C. J. Biol. Chem. *266*, 15771–15781.

Ullian, E.M., Sapperstein, S.K., Christopherson, K.S., and Barres, B.A. (2001). Control of synapse number by glia. Science *291*, 657–660.

Whitfield, R.A., and Jacobson, B.S. (1999). The β1-integrin cytosolic domain optimizes phospholipase A2-mediated arachidonic acid release required for NIH-3T3. Biochem. Biophys. Res. Commun. *258*, 306–312.

Yamaguchi, K., Tanaka, M., Mizoguchi, A., Hirata, Y., Ishizaki, H., Kaneko, K., Miyoshi, J., and Takai, Y. (2002). A GDP / GTP exchange protein for the Rab3 small G protein family up-regulates a postdocking step of synaptic exocytosis in central synapses. Proc. Natl. Acad. Sci. USA *99*, 14536–14541.

Yamamoto, H., Matsumura, T., Kugiyama, K., Oishi, Y., Ogata, N., Yasue, H., and Miyamoto, E. (1998). The antibody specific for myristoylated alanine-rich C kinase substrate phosphorylated by protein kinase C: activation of protein kinase C in smooth muscle cells in human coronary arteries. Arch. Biochem. Biophys. *359*, 151–159.